STRUCTURAL ANALYSIS OF BLAST RESISTANT BUILDINGS: TYPE AND BLAST LOAD CONSIDERATIONS

Mohammadmaruf Shakil Mulla¹, Dr.Sachin P Patil², Dr.Ravindra M Desai³

- [1] Department of Civil Engineering, Sanjay Ghodawat University, A/P Atigre, Kolhapur, Maharashtra 416118, INDIA
- [2] Department of Civil Engineering, Sanjay Ghodawat University, A/P Atigre, Kolhapur, Maharashtra 416118, INDIA
- [3] Department of Civil Engineering, Sanjay Ghodawat University A/P Atigre, Kolhapur, Maharashtra 416118, INDIA

ABSTRACT

This study investigates the structural response of G+15, G+20, and G+25 Reinforced Concrete (RCC) buildings subjected to blast loads, focusing on the vulnerability of buildings with soft storeys. The research utilizes Finite Element Analysis (FEA) and time-history simulations in ETABS to model the dynamic behavior of these buildings under various blast scenarios. The analysis incorporates blast load calculations based on the guidelines of IS 4991 and TM5-1300, considering key parameters such as peak overpressure, impulse duration, and reflected pressure. The study highlights that taller buildings, particularly those with soft storeys, exhibit greater displacement, drift, and overturning moments under blast loading. The G+25 model demonstrates the highest vulnerability to blast-induced forces, showing the most significant displacement and drift. The results emphasize the disproportionate failure of buildings with soft storeys, especially in taller structures, which leads to increased risk of collapse under blast conditions. Based on these findings, the study recommends strategies to enhance blast resistance, including reinforcing lower floors, incorporating shear walls, using blast-resistant materials, and implementing energy-dissipating devices. These recommendations aim to improve the resilience of buildings in high-risk environments, contributing to the development of safer, more robust infrastructure capable of withstanding explosive events.

Keywords: Blast load, structural response, soft storey, Finite Element Analysis, displacement, reinforcement.

I. INTRODUCTION

The study presented in the document focuses on the vulnerability of buildings to blast loads, particularly in high-risk zones such as defense facilities, petrochemical plants, and urban public spaces(Häring et al., 2020). This vulnerability is highlighted by the increased frequency of explosions due to terrorism, industrial accidents, and military conflicts. Traditional buildings, primarily designed to withstand static loads like dead and live loads, fail to provide sufficient resistance against the dynamic forces generated by blasts(Remennikov & Carolan, 2006). As a result, many high-rise buildings, especially those with soft storey conditions, face severe structural damage, leading to catastrophic failures. A soft storey, defined as a floor significantly weaker than adjacent floors, is especially vulnerable under lateral forces like those generated by seismic or blast events. The imbalance in lateral stiffness leads to excessive displacement and drift, which can cause severe collapse, particularly during explosive incidents. The study specifically targets the structural performance of G+15, G+20, and G+25 Reinforced Concrete (RCC) buildings subjected to blast loads(Syed et al., 2017). The primary aim is to assess the dynamic response of these buildings under various explosive scenarios, using advanced simulation techniques like Finite Element Analysis (FEA) and time-history simulations(Manohar & Raman, 2022).

The study employs blast load calculation methods outlined in IS 4991 and TM5-1300, which consider critical factors like peak overpressure, impulse, and reflected pressure(Anas et al., 2023). These calculations are crucial in understanding how these forces affect the structural behavior of the buildings, especially in terms of displacement, drift, overturning moments, and shear forces(Ngo et al., 2007). Initial results indicate that the taller the building, the more vulnerable it becomes to blast-induced forces(Mahmoud, 2014). The G+25 model, for example, demonstrates significantly higher displacement and drift, highlighting the greater susceptibility of taller buildings to such dynamic loads(Masi & Vona, 2012). In response to these findings, the study proposes several recommendations to improve the blast resistance of these buildings. These include reinforcing lower floors, incorporating shear walls, using blast-resistant materials, and implementing energy-dissipating devices(Gomes et al., 2024). Such interventions are designed to enhance the resilience of the structures, ensuring that they can withstand the growing threats posed by explosive events. Through this research, valuable insights are offered to guide the design of safer, more robust buildings,

particularly in high-risk environments. The ultimate goal is to bridge the gap left by traditional design approaches, contributing to the development of more resilient urban infrastructure(Barua et al., 2024).

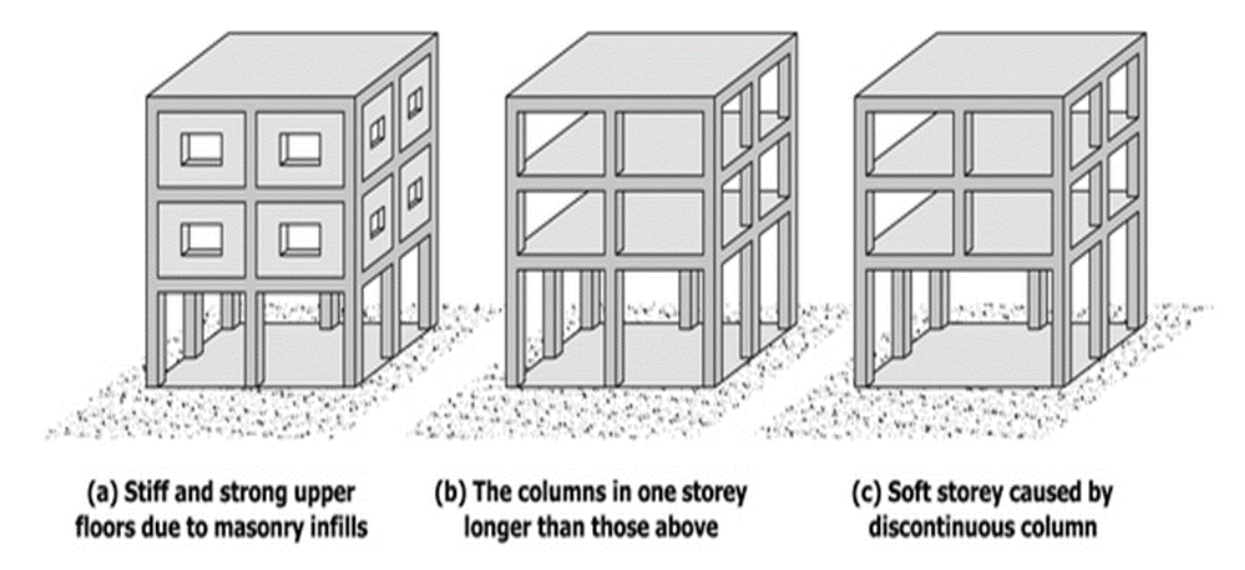


Figure 1. Effects of Column Discontinuity on Building Stiffness: (a) Stiff Upper Floors due to Masonry Infill, (b) Longer Columns in One Storey, (c) Soft Storey due to Discontinuous Column

1.1 Aim and Objectives

Aim

The aim of this study is to analyze and evaluate the structural behavior of various blast-resistant building types under different explosion scenarios, focusing on effective design strategies, material selection, and load modeling. The research seeks to develop comprehensive insights into blast load characteristics, simulate structural responses using advanced tools like finite element analysis (FEA), and propose optimized, cost-effective solutions for improving structural resilience against blasts.

Objectives

- To investigate the structural behavior of buildings subjected to blast loads.
- To categorize and analyze the different types of blast-resistant structures.
- To determine effective materials and structural systems for blast resistance.
- To study the application of analytical and simulation tools in assessing structural performance.
- To provide guidelines for integrating blast resistance into modern construction practices.

II. LITERATURE REVIEW

The study of blast-resistant buildings has garnered significant attention in recent years due to the rising threat of explosions from terrorism, industrial accidents, and military conflicts. Conventional buildings, designed to resist static loads such as dead and live loads, are inadequate in coping with the dynamic and short-duration forces generated by blasts. The response of multi-storey buildings, particularly those with soft storeys, has been of great concern in structural engineering(Zeynep Koccaz & Fatih Sutcu, 2008). A soft storey is characterized by reduced lateral stiffness compared to the floors above and below it, which makes it prone to failure under blast loads(Ngo et al., 2007). The vulnerability of buildings with soft storeys during explosive events has been documented in several studies. For instance, Biggs (1964) introduced dynamic structural response theory, which laid the foundation for later studies on blast loading(Mandal et al., 2022). His work emphasized the importance of analyzing buildings for dynamic loads rather than solely for static ones. Subsequent research by Krauthammer (1999) analyzed the failure mechanisms of slabs and walls under blast loads, which provided critical insights into the deformation and damage patterns of

structural elements exposed to explosive forces(Krauthammer, 1999). This work highlighted that traditional building codes do not account for the extreme pressures generated by blasts, necessitating advanced design strategies.

Further studies, such as those by Smith and Hetherington (2010), examined the material response to high strain rates during blasts, particularly focusing on the behavior of reinforced concrete under dynamic loading(Shi, 2014). They demonstrated that traditional materials such as concrete could be modified with additives, like fiber reinforcements, to enhance their resistance to blast forces. Similarly, the work of Luccioni et al. (2004) and Pham et al. (2013) used Finite Element Analysis (FEA) to simulate the behavior of structural systems under blast loads(Luccioni et al., 2004; Pham et al., 2018). Their research showed that numerical methods could effectively predict the dynamic response of buildings, thereby providing a tool for engineers to assess blast-induced damage. As blast resistance becomes increasingly crucial for civilian structures, there has been growing interest in developing and implementing innovative materials and design strategies. Ghani Razaqpur et al. (2018) and Yi et al. (2020) explored blast mitigation techniques, including sacrificial cladding, energy-absorbing devices, and progressive collapse prevention strategies(Hao et al., 2016). These studies emphasized that incorporating redundancy, ductility, and controlled failure modes were key to developing resilient structures. Moreover, Pargeter et al. (2017) and Usman et al. (2021) focused on the use of advanced materials, such as Carbon Fiber Reinforced Polymers (CFRPs), blast-resistant glazing, and layered wall systems, which have shown to significantly enhance the blast resistance of buildings(Q Rizwan & BK Raghu Prasad, 2017). These materials not only increase the structural strength but also improve the energy dissipation capacity, thus mitigating the effects of blasts.

Despite the advances in blast-resistant design, a critical gap remains in the standardization of blast-resistant building codes for civilian infrastructure. Jain and Srivastava (2020) argue that while defense-oriented standards, such as UFC 3-340-02, provide guidelines for blast-resistant structures, there is a need for region-specific guidelines that take into account local threats, construction practices, and material availability(Srivastava, 2022). Their research underscores the need for tailored approaches that account for the diverse environmental and construction conditions found in different parts of the world. In a similar vein, Kodur and Agarwal (2013) extended the study of blast loading to fullframe structures, examining failure modes such as buckling, joint failures, and disproportionate collapse under simulated blast conditions(Forni et al., 2017). They suggested that the performance of reinforced concrete buildings under blast loading could be significantly improved by incorporating progressive collapse mitigation strategies, which would prevent the structure from failing as a whole(Jayasooriya et al., 2011). Recent research has also explored the role of Finite Element Analysis (FEA) and advanced simulation tools in understanding the behavior of buildings under blast conditions. Numerical tools like ANSYS, ABAQUS, and LS-DYNA have become indispensable in simulating the effects of explosive forces on structures (Talaat et al., 2022). These computational tools help validate experimental data and provide engineers with a deeper understanding of how structures respond to extreme loading conditions (Luccioni et al., 2004; Pham et al., 2013). The ability to model and predict the dynamic response of buildings allows for more efficient and accurate design solutions to mitigate blast-induced damage(Pan et al., 2025).

Another important aspect of blast resistance is the evaluation of blast loads. Various methods have been developed to calculate the parameters that define the characteristics of a blast, such as peak overpressure, impulse duration, and reflected pressures. According to IS 4991 and TM5-1300, these parameters can be calculated using standard charts and formulas based on the scaled distance, which takes into account the distance between the blast source and the structure, as well as the explosive charge weight. Research by Jun-bao Li et al. (2023) and Yasser E. Ibrahim et al. (2019) has contributed to the development of blast load prediction models, improving the accuracy of these calculations(Ibrahim et al., 2024). The use of accurate blast load calculations is critical for simulating the impact of an explosion on a structure and for ensuring that buildings can withstand the pressures generated during such events. The integration of smart technologies, such as sensor networks and real-time monitoring systems, has also been proposed as a method to enhance the blast resistance of buildings. According to Zhang et al. (2020), the use of real-time data from these monitoring systems could provide immediate feedback on the performance of a building under blast loads, allowing for adaptive responses to mitigate damage(Zhang et al., 2020). This approach could complement traditional design strategies and offer a more dynamic and responsive solution to blast resistance(Sasi et al., 2021).

III. RESEARCH METHODOLOGY

The research methodology for this study focuses on analyzing the structural response of G+15, G+20, and G+25 Reinforced Concrete (RCC) buildings subjected to blast loads. The study employs a combination of blast load calculations, dynamic simulations, and Finite Element Analysis (FEA) to evaluate the behavior of these buildings under explosive forces.

Blast Load Calculation: The first step involves calculating the blast loads based on the guidelines provided in IS 4991 and TM5-1300. This includes determining key parameters such as peak overpressure, impulse duration, and reflected pressures. These parameters are derived using the scaled distance formula, which accounts for the distance between the blast source and the building, as well as the explosive charge weight. The TNT equivalent energy is calculated, and the resulting values for peak overpressure and impulse are applied to simulate the effects of the blast on the buildings.

Dynamic Simulation: Once the blast loads are determined, dynamic simulations are conducted using Finite Element Analysis (FEA) in ETABS. The study involves creating structural models of the buildings, which include the reinforcement details, material properties, and layout. The buildings are subjected to time-history simulations to model their response to the blast loads. Key parameters such as displacement, drift, shear forces, and overturning moments are evaluated for each building model under varying blast scenarios.

Model Validation: To ensure the accuracy of the simulation results, the model is validated against experimental data or known benchmarks from previous studies. This validation step helps to confirm that the numerical models accurately replicate the building's behavior under blast loading conditions.

Analysis and Recommendations: Finally, the results from the simulations are analyzed to identify critical vulnerabilities in the buildings. Based on these findings, recommendations are provided to enhance the blast resistance of the structures, including design modifications and material enhancements.

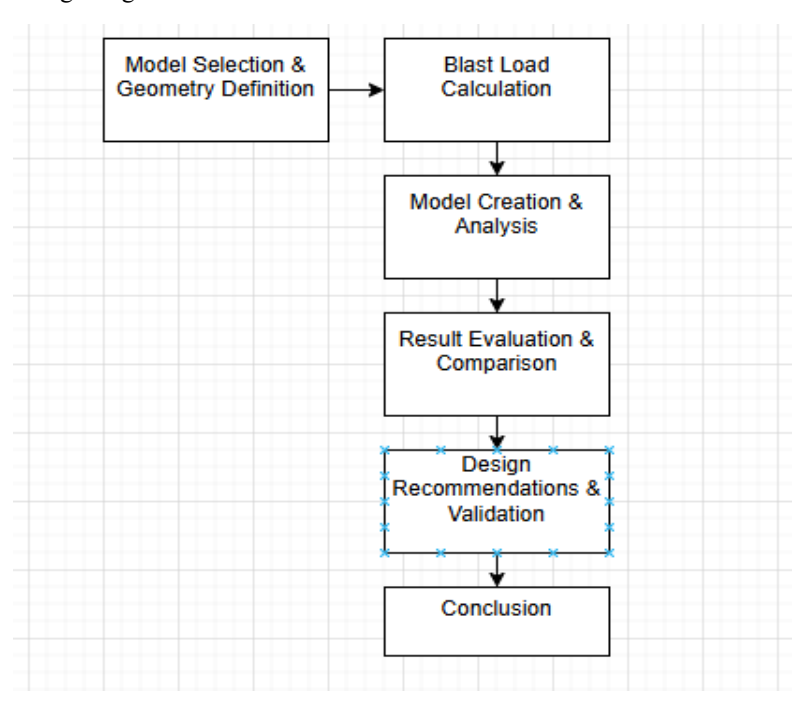


Figure 2. Methodology Flowchart for Blast Load Analysis and Structural Design Evaluation

IV. DESIGN AND MODELLING

The design and modeling of the G+15, G+20, and G+25 Reinforced Concrete (RCC) buildings subjected to blast loads involves several key steps to assess their structural performance under explosive forces. The process begins by defining the building geometry, including the number of storeys, storey height, and material properties. Each building model is assumed to be a moment-resisting frame with typical reinforcement detailing, and soft storey conditions are introduced in the lower floors to simulate realistic vulnerability. The modeling is conducted using Finite Element Analysis (FEA) in ETABS, where the building's structural elements—beams, columns, slabs, and shear walls—are represented using appropriate finite elements. The material properties of concrete (M30 grade) and steel (Fe500) are used, with the modulus of elasticity, yield strength, and Poisson's ratio for both materials being incorporated into the models.

V.Problem Statement

This research investigates the structural performance of G+15, G+20, and G+25 reinforced concrete buildings under blast loading, particularly focusing on buildings with soft storey irregularities and non-uniform shear wall distribution. Using IS:4991–1968 guidelines, the study models both regular and irregular buildings in ETABS to assess their vulnerability to blast-induced damage. It highlights the need for considering blast loads in addition to conventional gravity and seismic loads for buildings in sensitive zones, such as government offices and embassies.

• Beam sizes:

 \circ 300 mm \times 500 mm (up to 11th storey)

 \circ 250 mm \times 450 mm (top 4 storeys)

• Bay size: 3.15 m × 3.9 m

• Storey height: 3.6 m

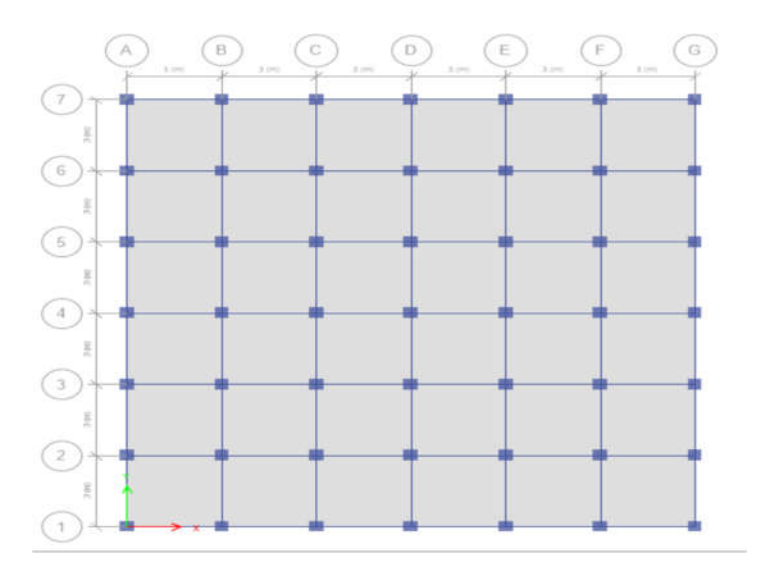
Grid Size 12m x 12m

• Slab thickness: 120 mm

Table no. 1: Storey Drift and Standoff Distance for Regular and Irregular Structures

TYPE	REGULAR STRUCTURE					
MODEL		STANDOFF DISTACE m				
G+15	10	15	20			
G+20	10	15	20			
G+25	10	15	20			
TYPE		IRREGULAR STRUCTURE				
MODEL		STANDOFF DISTACE m				
G+15	10	15	20			
G+20	10	15	20			
G+25	10	15	20			

As Mentioned in Above table, Total 18 models are analysed for TNT load 100 kg, Blast Load calculations are done using IS 4991 and later applied in ETABS



Graph 1: Storey Drift Analysis in EQ Y for Various Structural Scenarios

VI. Blast Load Calculation Based on IS:4991-1968

IS 4991:1968 provides guidance for calculating blast overpressures resulting from an explosion and converting them into equivalent static forces for structural design.

1. Scaled Distance (Z)

$$Z = \frac{R}{W^{1/3}}$$

Where:

- R = standoff distance (m)
- W = weight of TNT (kg)
- $Z = \text{scaled distance } (\text{m/kg}^{1/3})$

CASE 1: 100 kg TNT @ 10 m

Step 1: Scaled Distance Z

$$Z = \frac{R}{W^{1/3}} = \frac{10}{4.64} = 2.155$$

Step 2: Peak Reflected Pressure P_r

From blast chart at Z = 2.15:

$$P_r \approx 330.48 \,\mathrm{kN/m^2}$$

Step 3: Max Time t_d

From time-vs-Z chart for Z = 2.15:

$$t_d \approx 0.0036 \, \mathrm{sec}$$

CASE 2: 100 kg TNT @ 20 m

Step 1: Scaled Distance *Z*

$$Z = \frac{20}{4.64} = 4.31$$

Step 2: Peak Reflected Pressure P_r

From chart at Z = 4.31:

 $P_r \approx 148.08 \,\mathrm{kN/m}^2$

Step 3: Max Time t_d

From chart at Z = 4.31:

 $t_d \approx 0.0068 \, \mathrm{sec}$

CASE 3: 100 kg TNT @ 30 m

Step 1: Scaled Distance Z

$$Z = \frac{30}{4.64} = 6.47$$

Step 2: Peak Reflected Pressure P_r

From blast pressure chart at Z = 6.47:

$$P_r \approx 77 \, \text{kN/m}^2$$

Step 3: Max Time t_d

From positive phase duration chart at Z = 6.47:

$$t_d \approx 0.0096 \, \mathrm{sec}$$

Table no.2: Blast Impact Data for Different Distances

Case	Distance R (m)	$Z = \frac{R}{4.64}$	Pro (kN/m²)	Max Time (sec)
100 kg @ 10 m	10.0	2.155	330.48	0.0036
100 kg @ 20 m	20.0	4.310	148.08	0.0068
100 kg @ 30 m	30.0	6.470	77.00	0.0096

2. Peak Overpressure (Pr) Estimation

From IS 4991 Table 1 or UFC 3-340-02 chart (for $Z = 2.15 \text{ m/kg}^{1/3}$):

- Peak overpressure (Pr) ≈ 138 kPa
- Positive phase duration (td) $\approx 6.5 \text{ ms}$
- Impulse (I) $\approx 480 \text{ kPa} \cdot \text{ms}$

3. Equivalent Static Pressure (Peq)

As per IS:4991, the blast load can be modeled as an equivalent triangular load:

$$P_{\rm eq} = 0.5 \times P_r$$

$$P_{\rm eq} = 0.5 \times 138 = 69 \text{ kPa}$$

This is applied on the blast-exposed surface (typically ground floor exterior walls or façade).

4. Blast Load (Force) on Shear Wall

Assume exposed area (A) of a typical wall:

$$A = H \times L = 3.6 \times 21 = 75.6 \text{ m}^2$$

 $F = P_{eq} \times A = 69 \times 75.6 = 5,216.4 \text{ kN}$

This force is applied as lateral load on the first storey shear wall in the ETABS model.

Table no.3: Floor-wise Blast Impact Force Calculation

Floor	Center_Height (m)	Distance R (m)	Scaled Distance Z	Pro (kN/m^2)	Area (m^2)	Force (kN)
1	1.5	30.04	6.47	80	2.7	216
2	4.5	30.34	6.54	80	2.7	216
3	7.5	30.92	6.66	80	2.7	216
4	10.5	31.78	6.85	80	2.7	216
5	13.5	32.9	7.09	80	2.7	216
6	16.5	34.24	7.38	80	2.7	216
7	19.5	35.78	7.71	80	2.7	216
8	22.5	37.5	8.08	80	2.7	216
9	25.5	39.37	8.48	80	2.7	216
10	28.5	41.38	8.91	80	2.7	216
11	31.5	43.5	9.37	80	2.7	216
12	34.5	45.72	9.85	95	2.4	228
13	37.5	48.02	10.35	95	2.4	228
14	40.5	50.4	10.86	95	2.4	228
15	43.5	52.84	11.38	95	2.4	228

Table no. 4: Floor-wise Blast Load Impact Analysis

Floor	Center_Height (m)	Distance R (m)	Scaled Distance Z	Pro (kN/m^2)	Area (m^2)	Force (kN)
1	1.5	30.04	6.47	80	2.7	216
2	4.5	30.34	6.54	80	2.7	216
3	7.5	30.92	6.66	80	2.7	216
4	10.5	31.78	6.85	80	2.7	216

5	13.5	32.9	7.09	80	2.7	216
6	16.5	34.24	7.38	80	2.7	216
7	19.5	35.78	7.71	80	2.7	216
8	22.5	37.5	8.08	80	2.7	216
9	25.5	39.37	8.48	80	2.7	216
10	28.5	41.38	8.91	80	2.7	216
11	31.5	43.5	9.37	80	2.7	216
12	34.5	45.72	9.85	80	2.7	216
13	37.5	48.02	10.35	80	2.7	216
14	40.5	50.4	10.86	80	2.7	216
15	43.5	52.84	11.38	80	2.7	216
16	46.5	55.34	11.92	80	2.7	216
17	49.5	57.88	12.47	105	2.4	252
18	52.5	60.47	13.03	105	2.4	252
19	55.5	63.09	13.59	105	2.4	252
20	58.5	65.74	14.16	105	2.4	252
<u> </u>	1	I .	1	I .	1	1

Table no. 5: Floor-wise Blast Impact Force and Pressure Analysis

Floor	Center_Height (m)	Distance R (m)	Scaled Distance Z	Pro (kN/m^2)	Area (m^2)	Force (kN)
1	1.5	30.04	6.47	80	2.7	216
2	4.5	30.34	6.54	80	2.7	216
3	7.5	30.92	6.66	80	2.7	216
4	10.5	31.78	6.85	80	2.7	216
5	13.5	32.9	7.09	80	2.7	216
6	16.5	34.24	7.38	80	2.7	216
7	19.5	35.78	7.71	80	2.7	216
8	22.5	37.5	8.08	80	2.7	216
9	25.5	39.37	8.48	80	2.7	216
10	28.5	41.38	8.91	80	2.7	216
11	31.5	43.5	9.37	80	2.7	216
12	34.5	45.72	9.85	80	2.7	216

13	37.5	48.02	10.35	80	2.7	216
14	40.5	50.4	10.86	80	2.7	216
15	43.5	52.84	11.38	80	2.7	216
16	46.5	55.34	11.92	80	2.7	216
17	49.5	57.88	12.47	80	2.7	216
18	52.5	60.47	13.03	80	2.7	216
19	55.5	63.09	13.59	80	2.7	216
20	58.5	65.74	14.16	80	2.7	216
21	61.5	68.43	14.74	80	2.7	216
22	64.5	71.14	15.33	100	2.5	250
23	67.5	73.87	15.91	105	2.4	252
24	70.5	76.62	16.51	110	2.4	264
25	73.5	79.39	17.1	110	2.4	264

VII. Models in ETABS irregular

G+15 Regular and Irregular

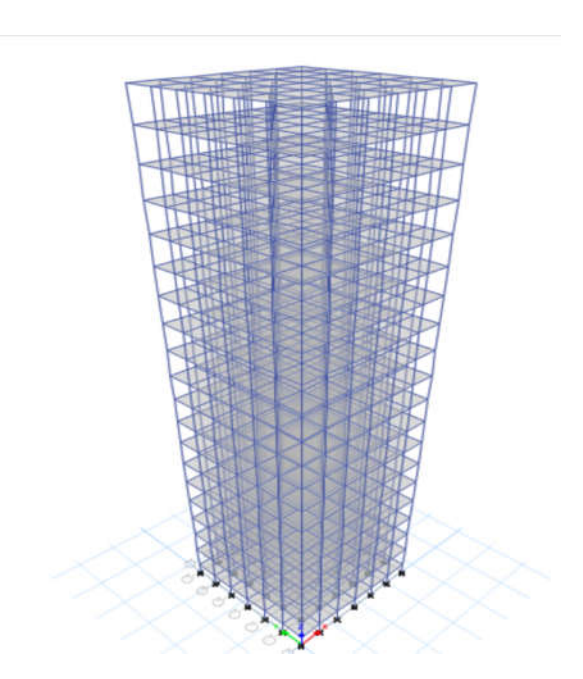


Figure 3:D Structural Frame Model of a High-Rise Building

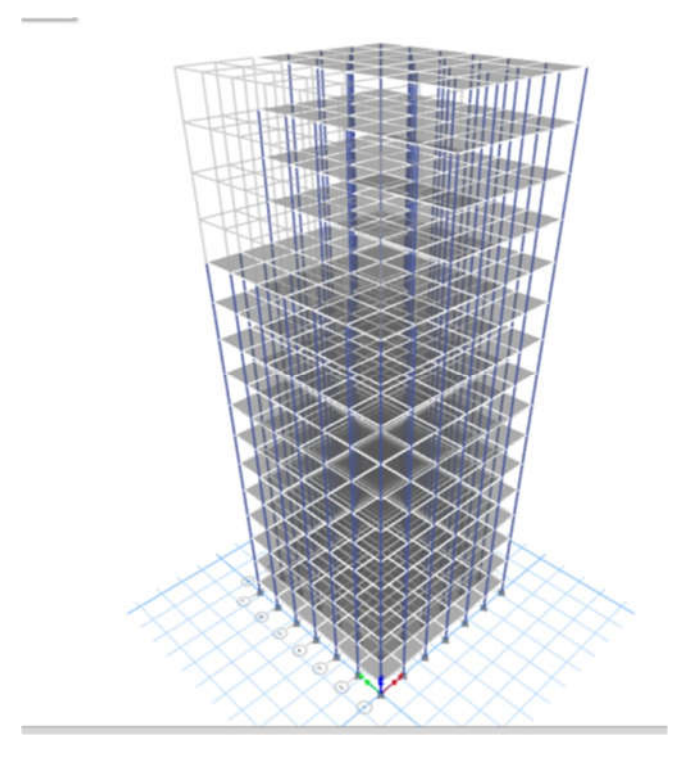


Figure 4: 3D Structural Model of the G+15 Building

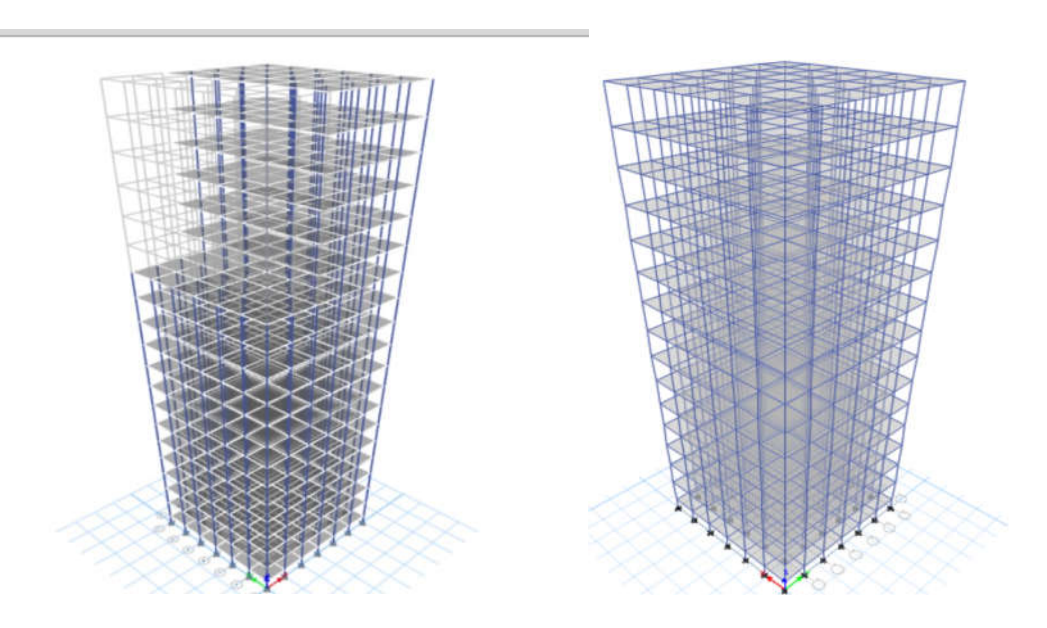


Figure 5: 3D and Elevation View of the Structural Model in ETABS

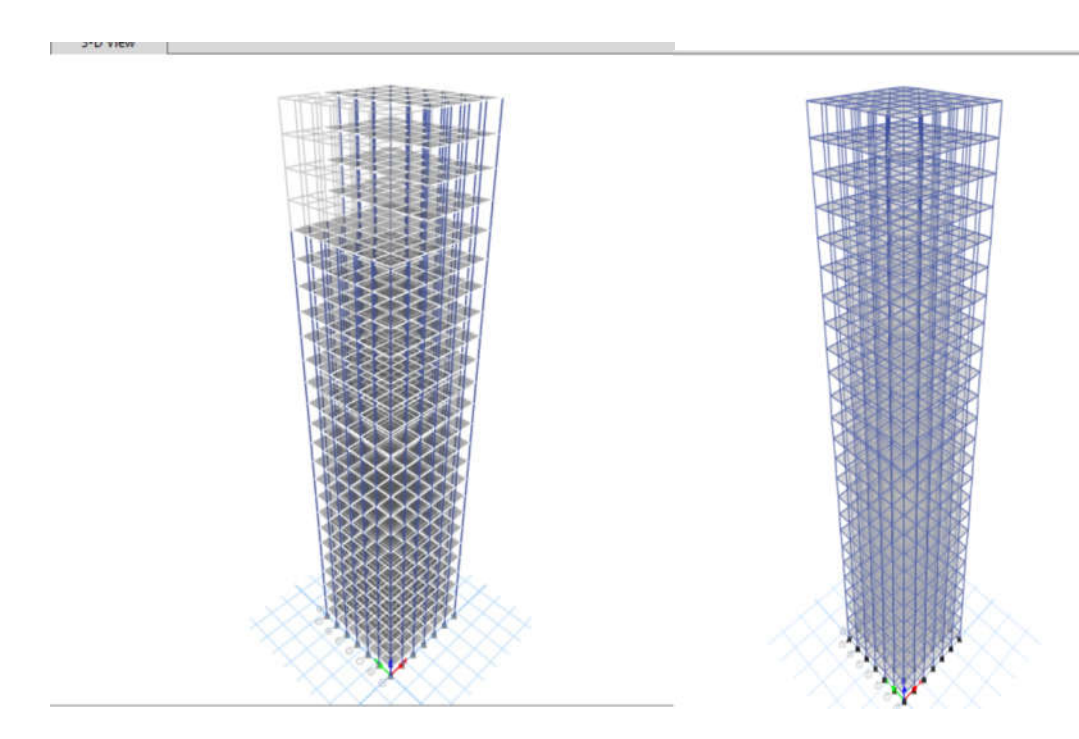


Figure 6 3D Structural Model of High-Rise Building

VIII. RESULT AND DESCUSSION

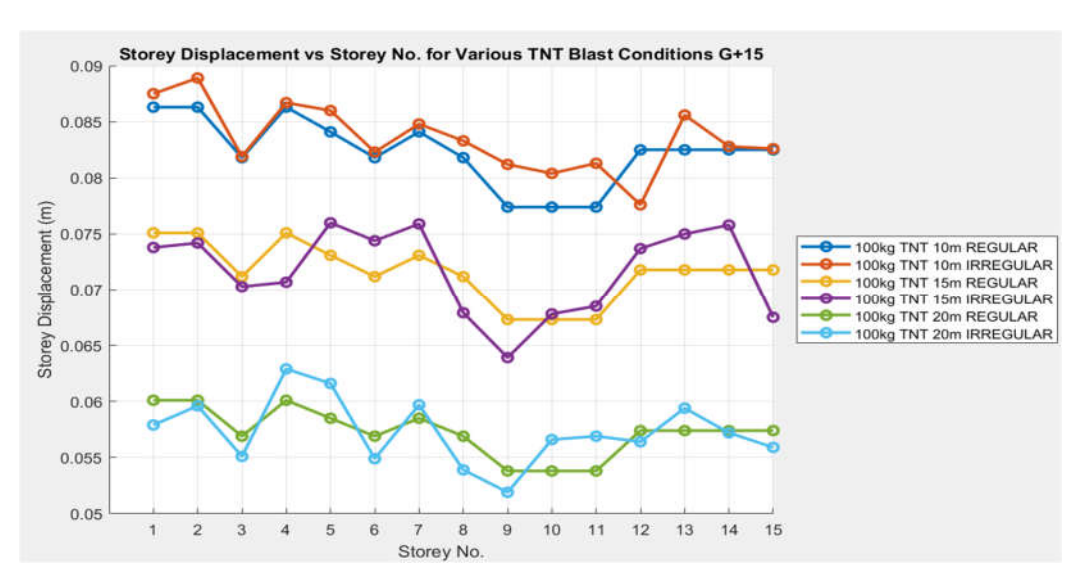
G+15

The table presents the deformation values for various TNT explosion scenarios (100 kg TNT) at different distances (10m, 15m, and 20m) and blast types (regular and irregular) across 15 storeys. The deformation values show a general decreasing trend as the distance from the explosion increases, with irregular blasts leading to slightly higher deformations compared to regular blasts. The deformation is highest at 10m and decreases with distance, indicating a reduction in impact with increasing proximity to the explosion source.

Table 6 Impact of TNT Explosion at Different Distances on Structural Deformation Across Storeys

STOREY NO.	100kg TNT 10m REGULAR	100kg TNT 10m IRREGULAR	100kg TNT 15m REGULAR	100kg TNT 15m IRREGULAR	100kg TNT 20m REGULAR	100kg TNT 20m IRREGULAR
1	0.0863	0.0875	0.0751	0.0738	0.0601	0.0579
2	0.0863	0.0889	0.0751	0.0742	0.0601	0.0596
3	0.0818	0.0819	0.0712	0.0703	0.0569	0.0551
4	0.0863	0.0867	0.0751	0.0707	0.0601	0.0629
5	0.0841	0.086	0.0731	0.076	0.0585	0.0616
6	0.0818	0.0823	0.0712	0.0744	0.0569	0.0549
7	0.0841	0.0848	0.0731	0.0759	0.0585	0.0597
8	0.0818	0.0833	0.0712	0.0679	0.0569	0.0539

9	0.0774	0.0812	0.0673	0.0639	0.0538	0.0519
10	0.0774	0.0804	0.0673	0.0678	0.0538	0.0566
11	0.0774	0.0813	0.0673	0.0685	0.0538	0.0569
12	0.0825	0.0776	0.0718	0.0737	0.0574	0.0564
13	0.0825	0.0856	0.0718	0.075	0.0574	0.0594
14	0.0825	0.0828	0.0718	0.0758	0.0574	0.0572
15	0.0825	0.0826	0.0718	0.0675	0.0574	0.0559



Graph 2 Storey Displacement vs Storey No. for Various TNT Blast Conditions G+15

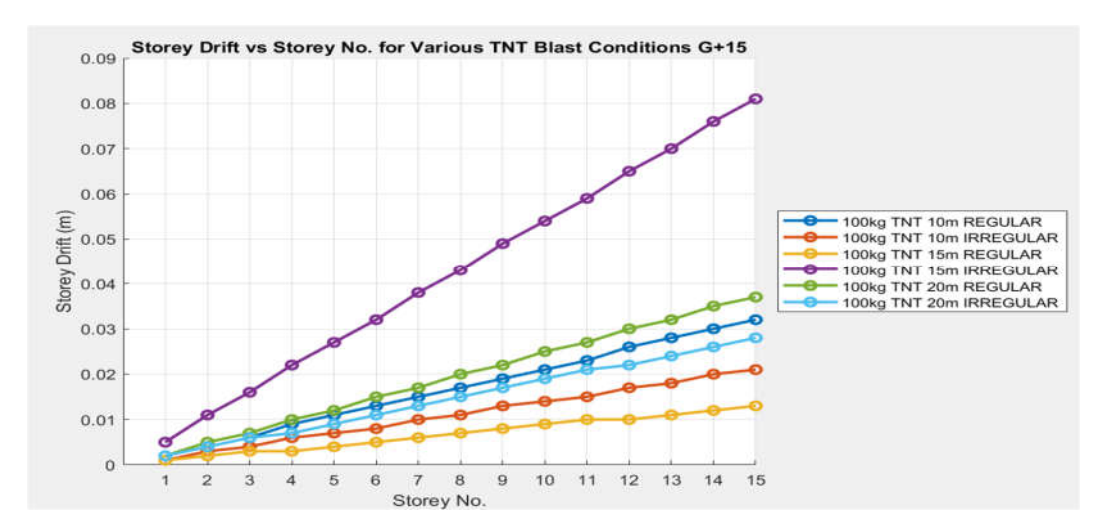
The graph shows the displacement of different storeys (1 to 15) under various TNT blast conditions (100kg TNT at different distances of 10m, 15m, and 20m for both regular and irregular conditions). The storey displacement is highest for the 100kg TNT at 10m in regular conditions, while the displacement decreases as the distance from the blast increases, with the lowest displacements observed at 20m under both regular and irregular blast conditions. The pattern of displacement fluctuations across the storeys is consistent, with slight variations as the blast distance changes.

This table illustrates the deformation values for various TNT blast scenarios (100 kg TNT) at distances of 10m, 15m, and 20m, and under regular and irregular blast conditions, across 15 storeys. As observed, the deformation increases with storey height, with the highest deformations occurring at the 15th storey. Additionally, irregular blasts lead to greater deformation than regular blasts at all distances. The deformation also reduces as the distance from the blast increases, with the highest deformations occurring at 10m and steadily decreasing at 15m and 20m. This data highlights the direct correlation between blast distance, blast irregularity, and structural response at varying storey heights

Table 7 Deformation of Structural Members under TNT Blast Load at Different Distances Across Storeys

STOREY NO.	100kg TNT 10m REGULAR	100kg TNT 10m IRREGULAR	100kg TNT 15m REGULAR	100kg TNT 15m IRREGULAR	100kg TNT 20m REGULAR	100kg TNT 20m IRREGULAR
1	0.002	0.001	0.001	0.005	0.002	0.002
2	0.004	0.003	0.002	0.011	0.005	0.004

3	0.006	0.004	0.003	0.016	0.007	0.006
4	0.009	0.006	0.003	0.022	0.01	0.007
5	0.011	0.007	0.004	0.027	0.012	0.009
6	0.013	0.008	0.005	0.032	0.015	0.011
7	0.015	0.01	0.006	0.038	0.017	0.013
8	0.017	0.011	0.007	0.043	0.02	0.015
9	0.019	0.013	0.008	0.049	0.022	0.017
10	0.021	0.014	0.009	0.054	0.025	0.019
11	0.023	0.015	0.01	0.059	0.027	0.021
12	0.026	0.017	0.01	0.065	0.03	0.022
13	0.028	0.018	0.011	0.07	0.032	0.024
14	0.03	0.02	0.012	0.076	0.035	0.026
15	0.032	0.021	0.013	0.081	0.037	0.028



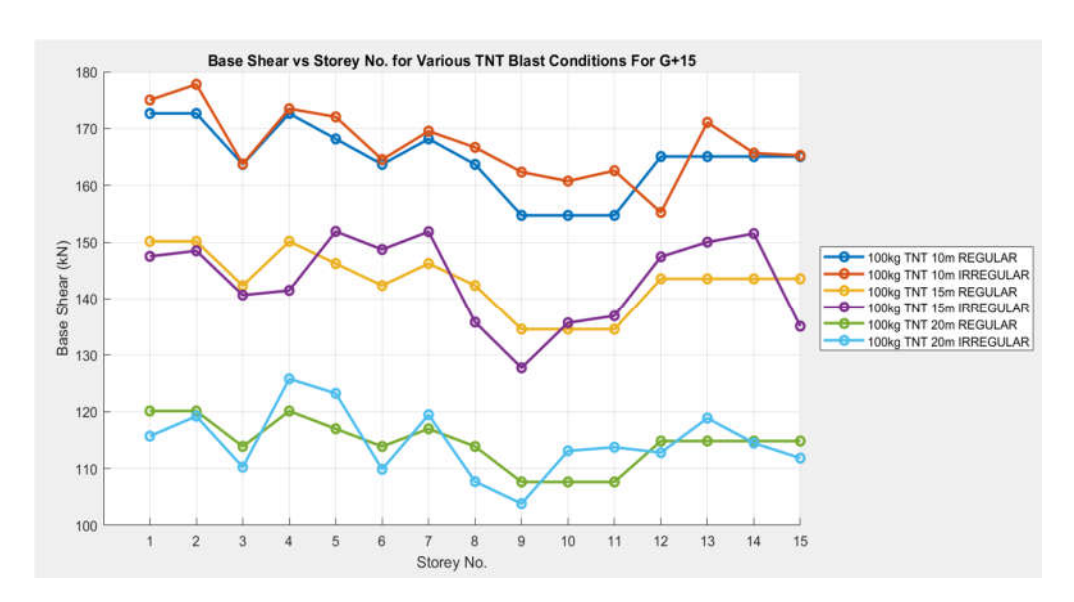
Graph 3 Storey Drift vs Storey No. for Various TNT Blast Conditions G+15

The graph illustrates the storey drift in response to varying TNT blast conditions at different distances (10m, 15m, and 20m) for a 100kg TNT explosion. It shows an increase in drift with the height of the building (storey number). For each distance, regular blast conditions exhibit higher storey drifts compared to irregular ones, with the drift magnitude rising with proximity to the explosion.

This table presents the structural responses (measured in deformation) at various storeys under TNT blast loads (100 kg TNT) at standoff distances of 10m, 15m, and 20m, with both regular and irregular blast conditions. The deformation values are highest at the 1st storey, decreasing gradually as the storey number increases. At each standoff distance, irregular blasts cause slightly higher deformation than regular blasts. As the standoff distance increases from 10m to 20m, the deformation values decrease, indicating a reduction in impact with increased distance from the blast source. The table shows a relatively consistent pattern across storeys, with irregular blasts consistently leading to more deformation than regular blasts at each distance.

Table 8 Structural Response to TNT Blast Loads at Various Standoff Distances and Blast Types

Standoff	100kg TNT 10m STANDOFF	100kg TNT 10m STANDOFF	100kg TNT 15m STANDOFF	100kg TNT 15m STANDOFF	100kg TNT 20m STANDOFF	100kg TNT 20m STANDOFF
STOREY NO.	REGULAR	IRREGULAR	REGULAR	IRREGULAR	REGULAR	IRREGULAR
1	172.67	175.04	150.15	147.52	120.12	115.71
2	172.67	177.79	150.15	148.49	120.12	119.21
3	163.7	163.76	142.35	140.67	113.88	110.24
4	172.67	173.5	150.15	141.5	120.12	125.79
5	168.19	172.07	146.25	151.9	117	123.24
6	163.7	164.55	142.35	148.72	113.88	109.86
7	168.19	169.55	146.25	151.86	117	119.47
8	163.7	166.69	142.35	135.8	113.88	107.71
9	154.73	162.35	134.55	127.73	107.64	103.82
10	154.73	160.76	134.55	135.68	107.64	113.11
11	154.73	162.6	134.55	136.92	107.64	113.75
12	165.08	155.25	143.55	147.44	114.84	112.8
13	165.08	171.1	143.55	150.02	114.84	118.88
14	165.08	165.69	143.55	151.52	114.84	114.48
15	165.08	165.26	143.55	135.07	114.84	111.83



Graph 4 Base Shear vs Storey No. for Various TNT Blast Conditions for G+15

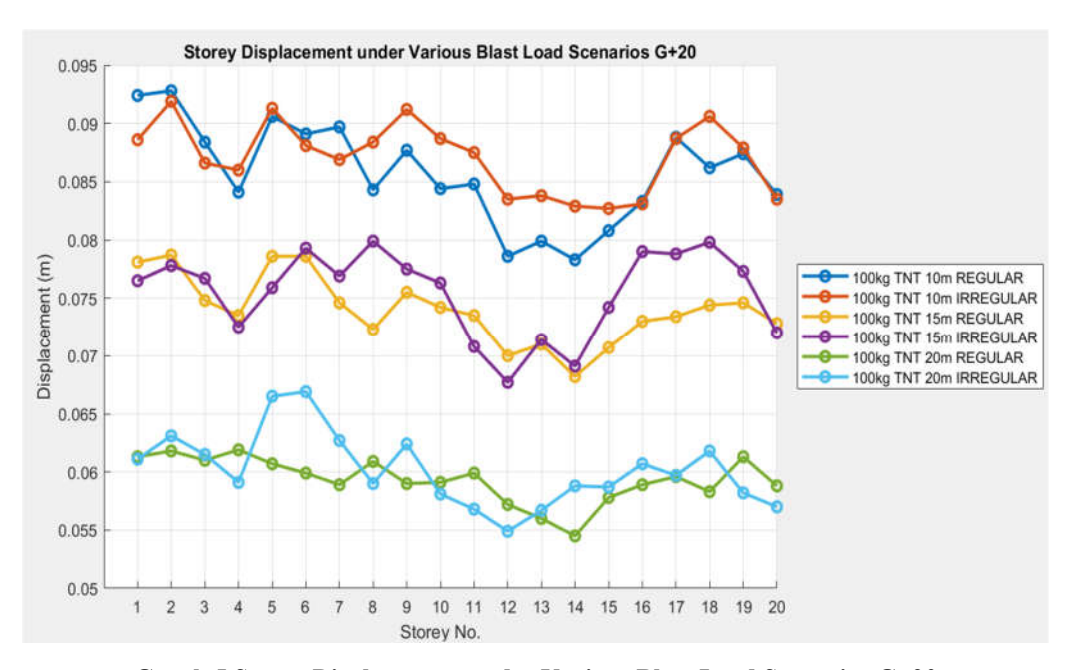
The graph illustrates the variation in base shear across different storeys (1 to 15) for various TNT blast conditions (100kg TNT at 10m, 15m, and 20m standoff distances) under regular and irregular scenarios. It shows that the base shear increases with the proximity of the blast (shorter standoff distance) and the irregularity of the structure. The base shear is highest for the 100kg TNT at 10m regular and irregular conditions, indicating more significant forces acting on the building closer to the blast.

G+20

This table presents the deformation values for various TNT blast scenarios (100 kg TNT) at distances of 10m, 15m, and 20m, under both regular and irregular blast conditions, across 20 storeys. The deformation values generally decrease as the distance from the blast increases, with the smallest deformations occurring at 20m. Irregular blasts result in slightly higher deformations compared to regular blasts at each distance. Deformation is highest at the 1st storey and decreases as the storey number increases. The data reveals a consistent pattern, where the impact of the explosion reduces with increasing distance from the blast source and irregular blasts lead to marginally more deformation than regular ones at all distances.

Table 9 Deformation of Structural Members Under TNT Blast Load at Varying Distances and Blast Types
Across Storeys

STOREY NO.	100kg TNT 10m REGULAR	100kg TNT 10m IRREGULAR	100kg TNT 15m REGULAR	100kg TNT 15m IRREGULAR	100kg TNT 20m REGULAR	100kg TNT 20m IRREGULAR
1	0.0924	0.0886	0.0781	0.0765	0.0613	0.0611
2	0.0928	0.0919	0.0787	0.0778	0.0618	0.0631
3	0.0884	0.0866	0.0748	0.0767	0.061	0.0615
4	0.0841	0.086	0.0735	0.0725	0.0619	0.0591
5	0.0906	0.0913	0.0786	0.0759	0.0607	0.0665
6	0.0891	0.0881	0.0786	0.0793	0.0599	0.0669
7	0.0897	0.0869	0.0746	0.0769	0.0589	0.0627
8	0.0843	0.0884	0.0723	0.0799	0.0609	0.059
9	0.0877	0.0912	0.0755	0.0775	0.059	0.0624
10	0.0844	0.0887	0.0742	0.0763	0.0591	0.0581
11	0.0848	0.0875	0.0735	0.0708	0.0599	0.0568
12	0.0786	0.0835	0.07	0.0677	0.0572	0.0549
13	0.0799	0.0838	0.071	0.0714	0.056	0.0567
14	0.0783	0.0829	0.0682	0.0691	0.0545	0.0588
15	0.0808	0.0827	0.0707	0.0742	0.0578	0.0587
16	0.0833	0.0831	0.073	0.079	0.0589	0.0607
17	0.0888	0.0887	0.0734	0.0788	0.0596	0.0597
18	0.0862	0.0906	0.0744	0.0798	0.0583	0.0618
19	0.0874	0.0879	0.0746	0.0773	0.0613	0.0582
20	0.0839	0.0835	0.0728	0.072	0.0588	0.057



Graph 5 Storey Displacement under Various Blast Load Scenarios G+20

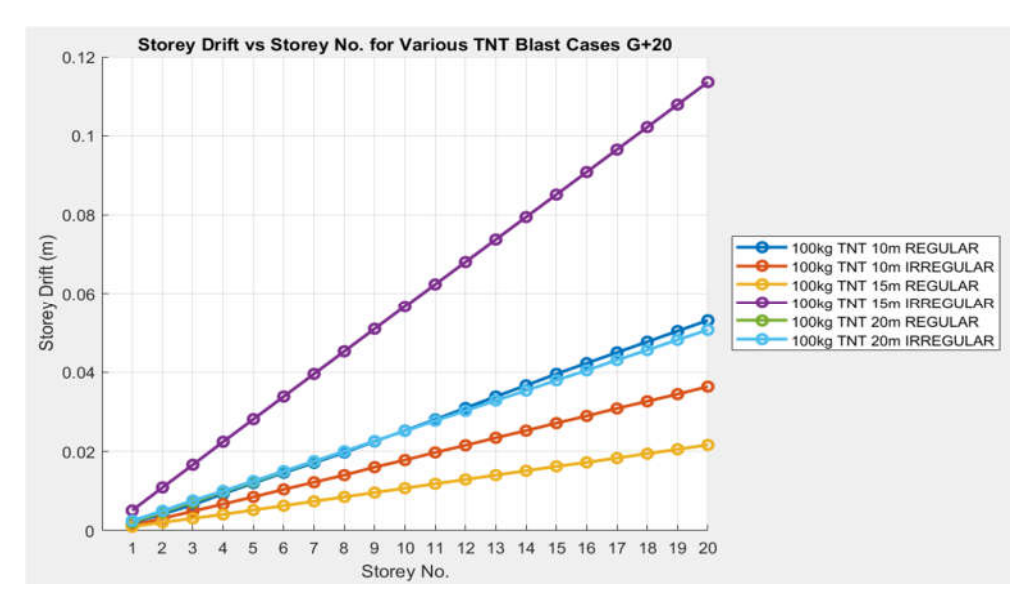
The graph shows the storey displacement values for different blast load scenarios involving 100kg TNT at varying distances (10m, 15m, 20m) and under both regular and irregular conditions. The displacement increases with a decrease in the blast load distance, indicating a higher response under closer blast loads. Irregular scenarios generally cause greater displacement compared to regular scenarios, showing that structural stability is more affected by irregular loading patterns. The displacement values peak in certain storeys, suggesting varying structural responses across different levels of the building.

This table shows the deformation values of structural members subjected to 100 kg TNT explosions at distances of 10m, 15m, and 20m, under both regular and irregular blast conditions, across 20 storeys. The deformation increases with storey height, with the maximum deformation observed at the 20th storey. The deformation is highest at 10m and decreases as the blast distance increases, with the lowest deformation at 20m. Irregular blasts consistently cause slightly higher deformation than regular blasts at all distances. This pattern reflects the increased intensity of the blast force closer to the source, with irregular blasts having a more pronounced effect on structural deformation.

Table 10 Deformation Response of Structural Members Under TNT Blast Load at Varying Distances and Blast Types Across Storeys

STOREY NO.	100kg TNT 10m REGULAR	100kg TNT 10m IRREGULAR	100kg TNT 15m REGULAR	100kg TNT 15m IRREGULAR	100kg TNT 20m REGULAR	100kg TNT 20m IRREGULAR
1	0.002	0.0013	0.001	0.0051	0.0021	0.0025
2	0.0042	0.0031	0.0021	0.0109	0.0047	0.005
3	0.0065	0.0049	0.0031	0.0166	0.0072	0.0076
4	0.0093	0.0067	0.0041	0.0224	0.0098	0.01
5	0.012	0.0085	0.0052	0.0281	0.0123	0.0125
6	0.0146	0.0104	0.0063	0.0338	0.0149	0.015

7	0.0171	0.0122	0.0074	0.0395	0.0174	0.0175
8	0.0197	0.014	0.0085	0.0452	0.02	0.02
9	0.0225	0.016	0.0096	0.0509	0.0226	0.0226
10	0.0252	0.0178	0.0107	0.0566	0.0251	0.0251
11	0.028	0.0197	0.0118	0.0623	0.0277	0.0277
12	0.0309	0.0215	0.0129	0.068	0.0302	0.0302
13	0.0338	0.0234	0.014	0.0737	0.0328	0.0328
14	0.0366	0.0252	0.0151	0.0794	0.0353	0.0353
15	0.0395	0.0271	0.0162	0.0851	0.0379	0.0379
16	0.0422	0.0289	0.0172	0.0908	0.0404	0.0404
17	0.0449	0.0308	0.0183	0.0965	0.043	0.043
18	0.0476	0.0326	0.0194	0.1022	0.0455	0.0455
19	0.0503	0.0344	0.0205	0.1079	0.0481	0.0481
20	0.053	0.0363	0.0216	0.1136	0.0506	0.0506



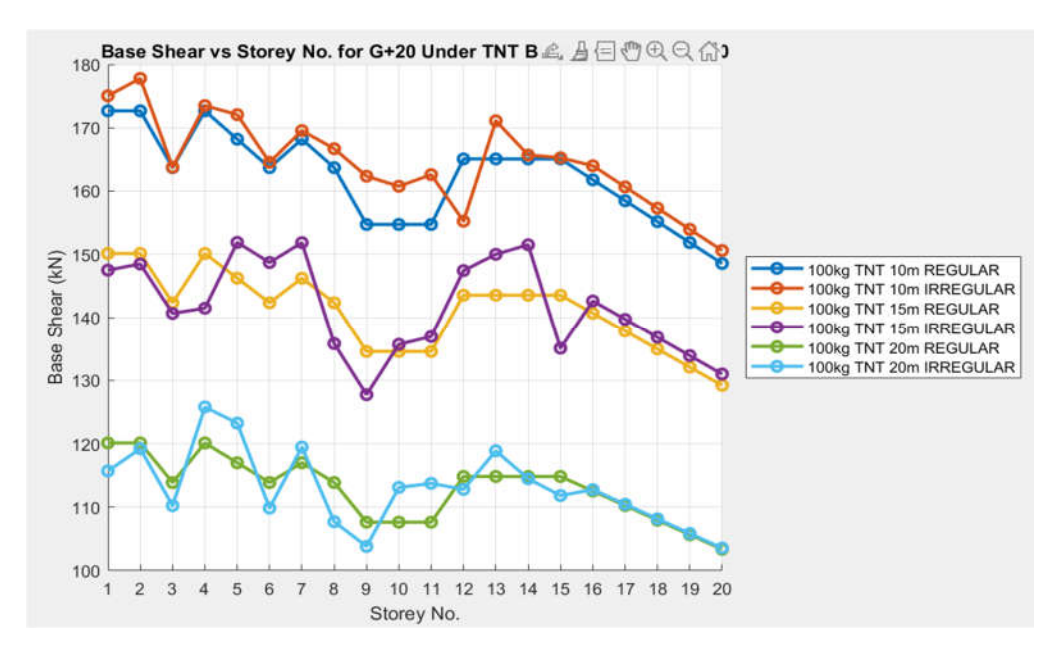
Graph 6 Storey Drift vs Storey No. for Various TNT Blast Cases G+20

This graph illustrates the storey drift of a building in response to TNT blast loads at different distances (10m, 15m, and 20m) and blast scenarios (regular and irregular). The storey drift increases with the number of storeys, and the drift is more pronounced for TNT at closer distances (10m), especially under irregular blast conditions. Irregular blasts consistently result in higher drift compared to regular blasts across all distances.

The table presents the deformation (in mm) of various storeys subjected to a 100kg TNT explosion at different standoff distances (10m, 15m, and 20m) for both regular and irregular blast scenarios. The deformation generally decreases with increased standoff distance, with the highest values occurring at 10m standoff distance, particularly for the regular explosion scenario. As the standoff distance increases, the blast impact on storey deformation diminishes, reflecting the reduced intensity of shockwaves at greater distances.

Table 11 Storey Deformation under TNT Explosion Impact at Different Standoff Distances

STOREY NO.	100kg TNT 10m STANDOFF - REGULAR	100kg TNT 10m STANDOFF - IRREGULAR	100kg TNT 15m STANDOFF - REGULAR	100kg TNT 15m STANDOFF - IRREGULAR	100kg TNT 20m STANDOFF - REGULAR	100kg TNT 20m STANDOFF - IRREGULAR
1	172.67	175.04	150.15	147.52	120.12	115.71
2	172.67	177.79	150.15	148.49	120.12	119.21
3	163.7	163.76	142.35	140.67	113.88	110.24
4	172.67	173.5	150.15	141.5	120.12	125.79
5	168.19	172.07	146.25	151.9	117	123.24
6	163.7	164.55	142.35	148.72	113.88	109.86
7	168.19	169.55	146.25	151.86	117	119.47
8	163.7	166.69	142.35	135.8	113.88	107.71
9	154.73	162.35	134.55	127.73	107.64	103.82
10	154.73	160.76	134.55	135.68	107.64	113.11
11	154.73	162.6	134.55	136.92	107.64	113.75
12	165.08	155.25	143.55	147.44	114.84	112.8
13	165.08	171.1	143.55	150.02	114.84	118.88
14	165.08	165.69	143.55	151.52	114.84	114.48
15	165.08	165.26	143.55	135.07	114.84	111.83
16	161.78	164	140.68	142.63	112.54	112.76
17	158.48	160.66	137.81	139.72	110.25	110.46
18	155.18	157.31	134.94	136.8	107.95	108.16
19	151.87	153.96	132.07	133.89	105.65	105.86
20	148.57	150.62	129.2	130.98	103.36	103.56



Graph 7 Base Shear vs Storey Number for G+20 Under TNT B.

This graph illustrates the variation in base shear across different storey numbers of a G+20 structure under TNT explosion loading at varying distances. The base shear decreases with increasing storey number, and there is a noticeable difference between the regular and irregular configurations for different TNT distances (10m, 15m, and 20m). Regular configurations generally exhibit higher base shear values compared to irregular configurations. Additionally, as the TNT distance increases, the base shear values tend to decrease across all configurations.

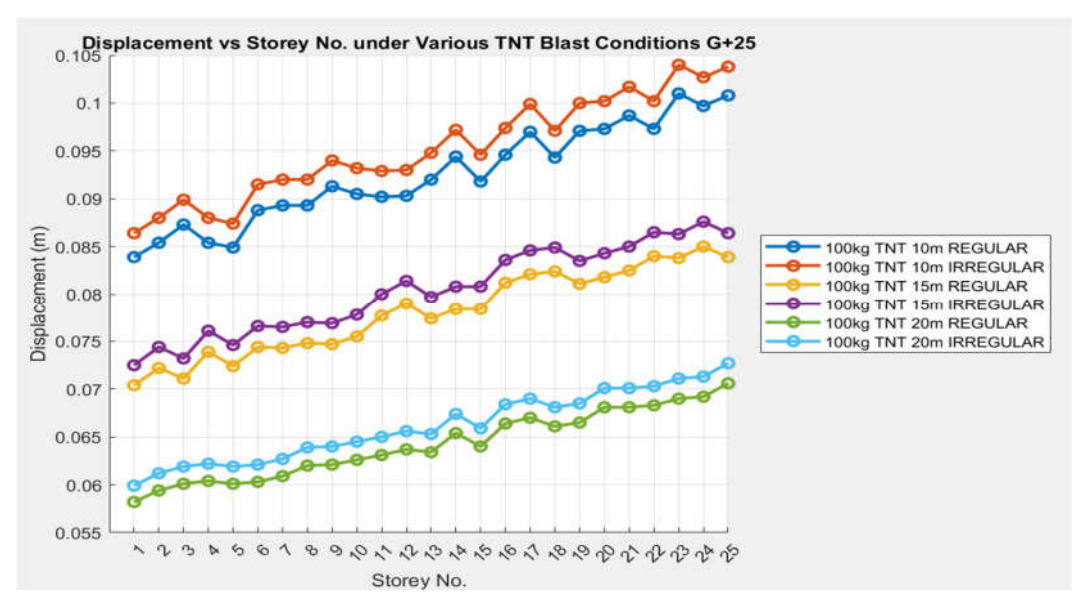
G+25

The table presents the displacement values (in meters) for various storeys subjected to a 100kg TNT explosion at different standoff distances (10m, 15m, and 20m) for both regular and irregular blast scenarios. As the standoff distance increases, the displacement values decrease across all storeys and both explosion scenarios. The highest displacements are observed at the 10m standoff distance, especially for the regular explosion scenario. The displacement values also tend to be higher in the irregular blast conditions compared to the regular ones, reflecting the greater intensity and irregularity of shockwaves in the former. Overall, the data highlights the inverse relationship between the standoff distance and displacement, with irregular blasts causing slightly higher displacement at each storey.

Table 12 Storey Displacement under TNT Explosion Impact at Different Standoff Distances

STOREY NO.	100kg TNT 10m REGULAR	100kg TNT 10m IRREGULAR	100kg TNT 15m REGULAR	100kg TNT 15m IRREGULAR	100kg TNT 20m REGULAR	100kg TNT 20m IRREGULAR
1	0.0839	0.0864	0.0704	0.0725	0.0582	0.0599
2	0.0854	0.088	0.0722	0.0744	0.0594	0.0612
3	0.0873	0.0899	0.0711	0.0732	0.0601	0.0619
4	0.0854	0.088	0.0739	0.0761	0.0604	0.0622
5	0.0849	0.0874	0.0724	0.0746	0.0601	0.0619
6	0.0888	0.0915	0.0744	0.0766	0.0603	0.0621

7	0.0893	0.092	0.0743	0.0765	0.0609	0.0627
8	0.0893	0.092	0.0748	0.077	0.062	0.0639
9	0.0913	0.094	0.0747	0.0769	0.0621	0.064
10	0.0905	0.0932	0.0755	0.0778	0.0626	0.0645
11	0.0902	0.0929	0.0777	0.08	0.0631	0.065
12	0.0903	0.093	0.079	0.0814	0.0637	0.0656
13	0.092	0.0948	0.0774	0.0797	0.0634	0.0653
14	0.0944	0.0972	0.0784	0.0808	0.0654	0.0674
15	0.0918	0.0946	0.0784	0.0808	0.064	0.0659
16	0.0946	0.0974	0.0812	0.0836	0.0664	0.0684
17	0.097	0.0999	0.0821	0.0846	0.067	0.069
18	0.0943	0.0971	0.0824	0.0849	0.0661	0.0681
19	0.0971	0.1	0.0811	0.0835	0.0665	0.0685
20	0.0973	0.1002	0.0818	0.0843	0.0681	0.0701
21	0.0987	0.1017	0.0825	0.085	0.0681	0.0701
22	0.0973	0.1002	0.084	0.0865	0.0683	0.0703
23	0.101	0.104	0.0838	0.0863	0.069	0.0711
24	0.0997	0.1027	0.085	0.0876	0.0692	0.0713
25	0.1008	0.1038	0.0839	0.0864	0.0706	0.0727



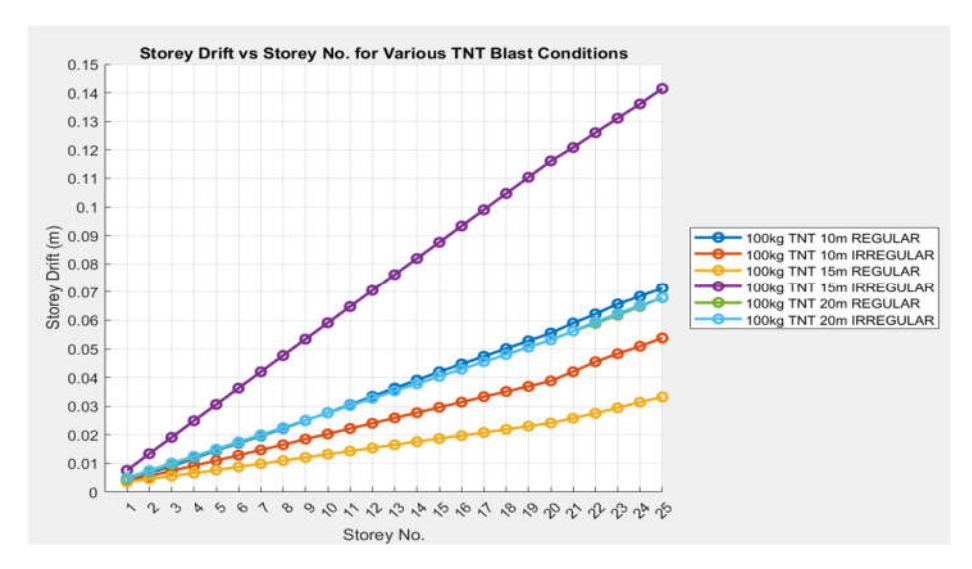
Graph 8 Displacement vs Storey No. under Various TNT Blast Conditions G+25

This figure illustrates the displacement of each storey under different TNT blast conditions (both regular and irregular) at varying distances (10m, 15m, and 20m). The displacement increases with the storey number and the TNT distance. The graph indicates that the displacement is more significant in the "irregular" blast conditions, especially at closer distances (10m). The trend is consistent across all blast scenarios, highlighting the impact of blast intensity on structural displacement.

This table shows the maximum acceleration (in m/s²) experienced by various storeys when subjected to a 100kg TNT explosion at different standoff distances (10m, 15m, and 20m) for both regular and irregular blast scenarios. As the standoff distance increases, the maximum acceleration values generally decrease, with the highest values recorded at the 10m standoff distance for both regular and irregular explosions. Additionally, irregular explosions produce slightly higher acceleration values compared to regular ones across all storeys. This indicates that irregular blasts exert a more intense force on the structure compared to regular blasts, especially at closer distances. The acceleration values increase progressively with storey height, showing a cumulative effect of the shockwave.

Table 13 Storey Maximum Acceleration under TNT Explosion Impact at Different Standoff Distances

STOREY NO.	100kg TNT 10m REGULAR	100kg TNT 10m IRREGULAR	100kg TNT 15m REGULAR	100kg TNT 15m IRREGULAR	100kg TNT 20m REGULAR	100kg TNT 20m IRREGULAR
1	0.0045	0.0038	0.0035	0.0076	0.0046	0.005
2	0.0067	0.0056	0.0046	0.0134	0.0072	0.0075
3	0.009	0.0074	0.0056	0.0191	0.0097	0.0101
4	0.0118	0.0092	0.0066	0.0249	0.0123	0.0125
5	0.0145	0.011	0.0077	0.0306	0.0148	0.015
6	0.0171	0.0129	0.0088	0.0363	0.0174	0.0175
7	0.0196	0.0147	0.0099	0.042	0.0199	0.02
8	0.0222	0.0165	0.011	0.0477	0.0225	0.0225
9	0.025	0.0185	0.0121	0.0534	0.0251	0.0251
10	0.0277	0.0203	0.0132	0.0591	0.0276	0.0276
11	0.0305	0.0222	0.0143	0.0648	0.0302	0.0302
12	0.0334	0.024	0.0154	0.0705	0.0327	0.0327
13	0.0363	0.0259	0.0165	0.0762	0.0353	0.0353
14	0.0391	0.0277	0.0176	0.0819	0.0378	0.0378
15	0.042	0.0296	0.0187	0.0876	0.0404	0.0404
16	0.0447	0.0314	0.0197	0.0933	0.0429	0.0429
17	0.0474	0.0333	0.0208	0.099	0.0455	0.0455
18	0.0501	0.0351	0.0219	0.1047	0.048	0.048
19	0.0528	0.0369	0.023	0.1104	0.0506	0.0506
20	0.0555	0.0388	0.0241	0.1161	0.0531	0.0531
21	0.059	0.042	0.0258	0.1208	0.0562	0.0562
22	0.0622	0.0455	0.0275	0.126	0.0589	0.0594
23	0.0657	0.0483	0.0294	0.1311	0.0618	0.0623
24	0.0684	0.0509	0.0314	0.1361	0.0648	0.0652
25	0.0713	0.0538	0.0332	0.1415	0.068	0.0679



Graph 9 Storey Drift vs Storey No. for Various TNT Blast Conditions

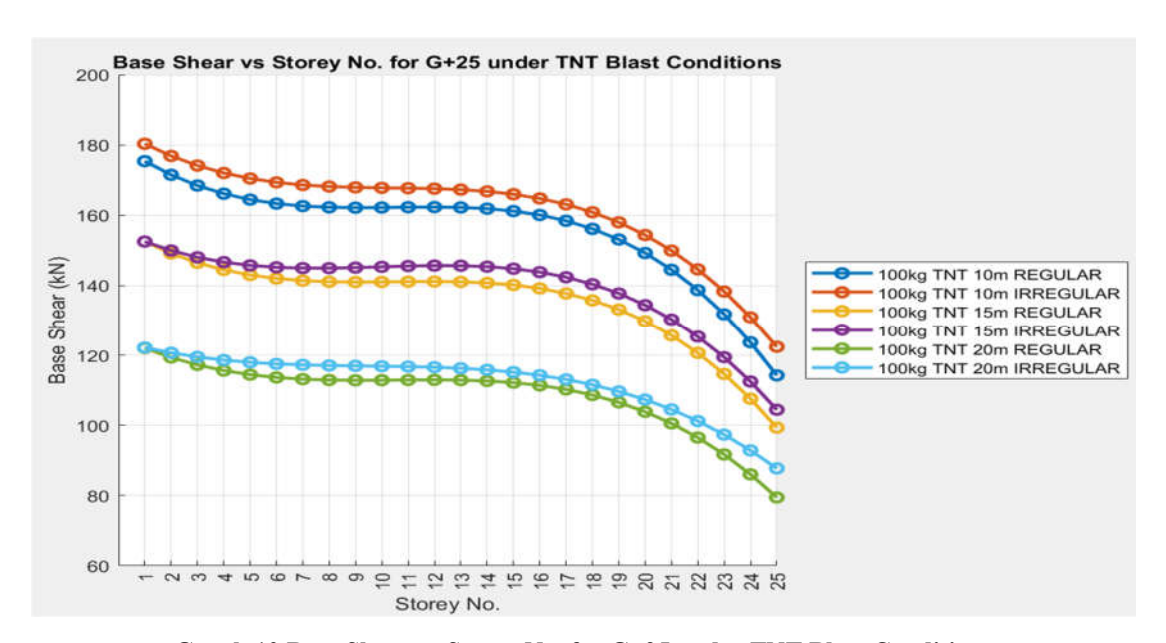
This graph illustrates the relationship between storey drift and storey number for different TNT blast conditions (at 10m, 15m, and 20m distances). It shows a clear increase in storey drift as the storey number rises. The drift increases more rapidly with irregular blast conditions compared to regular ones, with higher TNT quantities (e.g., 100kg at 20m) leading to greater storey displacements. The results suggest that building deformation under explosive forces varies with both the distance of the blast and the nature of the blast (regular vs irregular).

This table presents the storey displacement (in mm) under the impact of a 100kg TNT explosion at various standoff distances (10m, 15m, and 20m) for both regular and irregular explosion scenarios. The displacement decreases as the standoff distance increases, with the highest values observed at a 10m standoff, particularly for the regular explosion. Irregular explosions result in slightly higher displacement values compared to regular ones at each standoff distance. The displacement values gradually decrease as the storey number increases, showing that the higher storeys experience less displacement compared to the lower ones. This trend highlights the inverse relationship between standoff distance and displacement, with irregular explosions causing slightly more structural deformation than regular blasts at each distance.

Table 14 Storey Displacement under TNT Explosion Impact at Different Standoff Distances (Impact in mm)

STOREY NO.	100kg TNT 10m STANDOFF - REGULAR	100kg TNT 10m STANDOFF - IRREGULAR	100kg TNT 15m STANDOFF - REGULAR	100kg TNT 15m STANDOFF - IRREGULAR	100kg TNT 20m STANDOFF - REGULAR	100kg TNT 20m STANDOFF - IRREGULAR
1	175.4	180.34	152.53	152.54	122.02	122.18
2	171.52	176.89	149.15	150	119.32	120.66
3	168.47	174.15	146.5	148.07	117.2	119.48
4	166.16	172.04	144.49	146.69	115.59	118.59
5	164.48	170.48	143.03	145.77	114.42	117.95
6	163.34	169.37	142.04	145.23	113.63	117.5
7	162.64	168.63	141.43	145	113.14	117.22

8	162.29	168.19	141.12	144.99	112.9	117.04
9	162.18	167.95	141.03	145.14	112.82	116.93
10	162.22	167.82	141.06	145.36	112.85	116.84
11	162.31	167.73	141.14	145.58	112.91	116.72
12	162.35	167.59	141.18	145.71	112.94	116.55
13	162.25	167.31	141.09	145.68	112.87	116.25
14	161.91	166.81	140.79	145.41	112.63	115.8
15	161.22	166	140.2	144.83	112.16	115.15
16	160.1	164.8	139.22	143.85	111.38	114.26
17	158.45	163.13	137.78	142.4	110.22	113.07
18	156.16	160.89	135.79	140.4	108.63	111.55
19	153.14	158.01	133.17	137.77	106.53	109.64
20	149.29	154.4	129.83	134.43	103.86	107.32
21	144.52	149.97	125.68	130.31	100.54	104.52
22	138.72	144.64	120.64	125.33	96.51	101.21
23	131.81	138.32	114.63	119.41	91.7	97.34
24	123.67	130.94	107.56	112.47	86.04	92.86
25	114.22	122.39	99.34	104.43	79.47	87.74



Graph 10 Base Shear vs Storey No. for G+25 under TNT Blast Conditions

This figure presents the base shear (in kN) versus storey number for a G+25 building subjected to various TNT blast conditions. The graph shows that the base shear decreases as the storey number increases, with the irregular blast conditions (represented by orange, purple, and green lines) causing higher base shear values compared to regular blast conditions (represented by blue, purple, and green lines). Additionally, the TNT blast intensity (10m, 15m, 20m stand-off distances) has a noticeable impact, with closer stand-off distances (10m) resulting in higher base shear forces.

Time and Frequency

Cases	Max time (sec)	Front Face Max Load (kN/m²)
100kg @ 30m	0.0058	150.15

Table no.15 Mode Shape, Time Period, and Frequency Data

Time period (sec)	Frequency	
1.2	0.833	
1.13	0.885	
1.06	0.943	
0.99	1.01	
0.92	1.087	
0.85	1.176	
0.78	1.282	
0.71	1.408	
0.64	1.562	
0.57	1.754	
0.5	2	
0.43	2.326	
0.36	2.778	
0.29	3.448	
0.22	4.545	
	1.2 1.13 1.06 0.99 0.92 0.85 0.78 0.71 0.64 0.57 0.5 0.43 0.36 0.29	1.2 0.833 1.13 0.885 1.06 0.943 0.99 1.01 0.92 1.087 0.85 1.176 0.78 1.282 0.71 1.408 0.64 1.562 0.57 1.754 0.5 2 0.43 2.326 0.36 2.778 0.29 3.448

Table no.16 Mode Shape, Time Period, and Frequency Data (Second Set)

Mode Shape No	Time period (sec)	Frequency
1	1.3	0.769
2	1.245	0.803
3	1.19	0.84
4	1.135	0.881
5	1.08	0.926
6	1.025	0.976
7	0.97	1.031
8	0.915	1.093

9	0.86	1.163
10	0.805	1.242
11	0.75	1.333
12	0.695	1.439
13	0.64	1.562
14	0.585	1.709
15	0.53	1.887
16	0.475	2.105
17	0.42	2.381
18	0.365	2.74
19	0.31	3.226
20	0.255	3.922

Table no 17. Mode Shape, Time Period, and Frequency Data (Third Set)

Mode Shape No	Time period (sec)	Frequency
1	1.4	0.714
2	1.352	0.74
3	1.304	0.767
4	1.256	0.796
5	1.208	0.828
6	1.16	0.862
7	1.112	0.899
8	1.064	0.94
9	1.016	0.984
10	0.968	1.033
11	0.92	1.087
12	0.872	1.147
13	0.824	1.214
14	0.776	1.289
15	0.728	1.374
16	0.68	1.471
17	0.632	1.582
18	0.584	1.712
19	0.536	1.866
20	0.488	2.049
21	0.44	2.273
22	0.392	2.551
23	0.344	2.907
24	0.296	3.378
25	0.248	4.032

IX. CONCLUSION

In conclusion, this study provides a comprehensive analysis of the structural response of G+15, G+20, and G+25 Reinforced Concrete (RCC) buildings subjected to blast loads. The findings highlight the significant vulnerability of taller buildings, particularly those with soft storeys, to blast-induced forces. The use of Finite Element Analysis (FEA) and time-history simulations in ETABS has demonstrated the increased displacement, drift, and overturning moments as the building height increases, with the G+25 model showing the highest vulnerability. The study underscores the importance of considering dynamic loads, such as blast forces, in building design, as traditional static load methodologies are insufficient to account for the intense and short-duration forces generated by explosions. The results reveal that soft storeys contribute disproportionately to failure under blast conditions, particularly in taller buildings.

Based on these findings, several recommendations are made to improve blast resistance, including reinforcing lower floors, incorporating shear walls, utilizing blast-resistant materials, and implementing energy-dissipating devices. These strategies are crucial for enhancing the resilience of high-rise buildings, particularly in high-risk zones prone to explosions. Overall, the study contributes valuable insights into the design of safer and more resilient structures, offering practical guidelines for improving the blast resistance of buildings in blast-prone environments.

X. FUTURE SCOPE

The future scope of this research lies in expanding the analysis to further enhance the design and resilience of buildings subjected to blast loads. One key area for future exploration is the incorporation of multi-hazard scenarios, considering the combined effects of blast loads with other dynamic forces such as seismic and wind loads. This would provide a more comprehensive understanding of a building's performance under real-world conditions, where multiple hazards may occur simultaneously. Additionally, the study could benefit from experimental validation, where real-scale testing of blast-resistant structures is conducted to verify the accuracy of the simulation results. This would help improve the reliability of predictive models and provide a deeper understanding of the physical response of buildings under extreme conditions.

Research into advanced materials and retrofitting techniques also holds significant potential. The use of ultra-high-performance concrete (UHPC), carbon fiber-reinforced polymers (CFRPs), and other innovative materials could further improve blast resistance. Furthermore, retrofitting existing buildings with modern blast-resistant solutions can contribute to enhancing the safety of older structures in high-risk areas. The development of performance-based design criteria tailored to specific threat levels could also be explored, offering cost-effective and customized solutions for blast mitigation. Lastly, integrating smart technologies like real-time monitoring and sensor networks could provide valuable data for dynamic response evaluation and rapid damage assessment during blast events.

XI. REFERENCES

- Anas, S. M., Alam, M., & Umair, M. (2023). Reinforced cement concrete (RCC) shelter and prediction of its blast loads capacity. *Materials Today: Proceedings*, 74, 547–568. https://doi.org/10.1016/j.matpr.2022.09.125
- 2. Barua, U., Han, H., Mojtahedi, M., & Ansary, M. A. (2024). Integration of Proactive Building Fire Risk Management in the Building Construction Sector: A Conceptual Framework to Understand the Existing Condition. *Buildings*, 14(11), 3372. https://doi.org/10.3390/buildings14113372
- 3. Forni, D., Chiaia, B., & Cadoni, E. (2017). Blast effects on steel columns under fire conditions. *Journal of Constructional Steel Research*, 136, 1–10. https://doi.org/10.1016/j.jcsr.2017.04.012
- 4. Gomes, G. D. J., Lúcio, V. J. D. G., & Cismasiu, C. (2024). Development of a high-performance blast energy-absorbing system for building structures. *International Journal of Protective Structures*, *15*(3), 484–508. https://doi.org/10.1177/20414196231183006
- 5. Hao, H., Hao, Y., Li, J., & Chen, W. (2016). Review of the current practices in blast-resistant analysis and design of concrete structures. *Advances in Structural Engineering*, 19(8), 1193–1223. https://doi.org/10.1177/1369433216656430
- 6. Häring, I., Pfeiffer, M., Vogelbacher, G., Stottmeister, A., Restayn, E.-M., Ross, K., & Ramin, M. V. (2020). Risk and Resilience Analysis of Public Civil Buildings Against Shelling with Explosive Sources in

- Urban Contexts. European Journal for Security Research, 5(2), 311–347. https://doi.org/10.1007/s41125-019-00046-9
- Ibrahim, M. T., Eisa, A. S., Elshazli, M. T., Yasser E., & El-Zohairy, A. (2024). Numerical Analysis of Rubberized Steel Fiber Reinforced Concrete Beams Subjected to Static and Blast Loadings. *Infrastructures*, 9(3), 52. https://doi.org/10.3390/infrastructures9030052
- 8. Jayasooriya, R., Thambiratnam, D. P., Perera, N. J., & Kosse, V. (2011). Blast and residual capacity analysis of reinforced concrete framed buildings. *Engineering Structures*, *33*(12), 3483–3495. https://doi.org/10.1016/j.engstruct.2011.07.011
- 9. Krauthammer, T. (1999). Blast-resistant structural concrete and steel connections. *International Journal of Impact Engineering*, 22(9–10), 887–910. https://doi.org/10.1016/S0734-743X(99)00009-3
- 10. Luccioni, B. M., Ambrosini, R. D., & Danesi, R. F. (2004). Analysis of building collapse under blast loads. *Engineering Structures*, 26(1), 63–71. https://doi.org/10.1016/j.engstruct.2003.08.011
- 11. Mahmoud, S. (2014). Blast load induced response and the associated damage of buildings considering SSI. *Earthquakes and Structures*, 7(3), 349–365. https://doi.org/10.12989/EAS.2014.7.3.349
- 12. Mandal, J., Goel, M. D., & Agarwal, A. K. (2022). Underground Structures Subjected to Various Blast Loading Scenarios: A Scoping Review. *Archives of Computational Methods in Engineering*, 29(4), 2491–2512. https://doi.org/10.1007/s11831-021-09664-w
- 13. Manohar, A., & Raman, A. (2022). Study of Blast Load and Blast Resistant Building. *International Journal of Engineering Research*, 10(06).
- 14. Masi, A., & Vona, M. (2012). Vulnerability assessment of gravity-load designed RC buildings: Evaluation of seismic capacity through non-linear dynamic analyses. *Engineering Structures*, *45*, 257–269. https://doi.org/10.1016/j.engstruct.2012.06.043
- 15. Ngo, T., Mendis, P., A. Gupta, & J. Ramsay. (2007). Blast Loading and Blast Effects on Structures An Overview. *Electronic Journal of Structural Engineering*, 1, 76–91. https://doi.org/10.56748/ejse.671
- 16. Pan, J., Zhang, D., Zhou, Z., He, J., Zhang, L., Han, Y., Peng, C., & Wang, S. (2025). Experimental Study on Dynamic Response Characteristics of Rural Residential Buildings Subjected to Blast-Induced Vibrations.
- 17. Pham, T. M., Chen, W., & Hao, H. (2018). Failure and impact resistance analysis of plain and fiber-reinforced-polymer confined concrete cylinders under axial impact loads. *International Journal of Protective Structures*, 9(1), 4–23. https://doi.org/10.1177/2041419617749600
- 18. Q Rizwan & BK Raghu Prasad. (2017). Structural analysis of Blast Resistant buildings. https://www.ijrdt.org/upload/6951129-Structural%20analysis%20of%20Blast%20Resistant%20buildings.pdf
- 19. Remennikov, A., & Carolan, D. (2006). Blast Effects and Vulnerability of Building Structures from Terrorist Attack. *Australian Journal of Structural Engineering*, 7(1), 1–11. https://doi.org/10.1080/13287982.2006.11464959
- 20. Sasi, D., Joy, J., Thomas, M. M., & Thomas, N. U. (2021). Prediction of blast loading and its effect on RCC structures. 08(06).
- 21. Shi, Y. (2014). Spatial Reliability Analysis of Reinforced Concrete Structures Subject to Explosive Blast Loading. https://doi.org/file:///C:/Users/Admin/Downloads/Thesis_ATTACHMENT02.pdf
- 22. Srivastava, S., & Gaurav. (2022). Fire-Resistant Design of Structures (1st ed.). CRC Press. https://doi.org/10.1201/9781003328711
- 23. Syed, Z. I., Mohamed, O. A., Murad, K., & Kewalramani, M. (2017). Performance of Earthquake-resistant RCC Frame Structures under Blast Explosions. *Procedia Engineering*, *180*, 82–90. https://doi.org/10.1016/j.proeng.2017.04.167
- 24. Talaat, M., Yehia, E., Mazek, S. A., Genidi, M. M. M., & Sherif, A. G. (2022). Finite element analysis of RC buildings subjected to blast loading. *Ain Shams Engineering Journal*, *13*(4), 101689. https://doi.org/10.1016/j.asej.2021.101689
- 25. Zeynep Koccaz & Fatih Sutcu. (2008). *BLAST RESISTANT BUILDING DESIGN*. https://www.iitk.ac.in/nicee/wcee/article/14 05-01-0536.PDF
- 26. Zhang, J., Zhou, Y., Rui, Liu, C., & Zhang, Z. (2020). Numerical simulation of reinforced concrete slab subjected to blast loading and the structural damage assessment. *Engineering Failure Analysis*, 118, 104926. https://doi.org/10.1016/j.engfailanal.2020.104926